This is an open access article published under an ACS AuthorChoice License, which permits copying and redistribution of the article or any adaptations for non-commercial purposes.

ACS OMEGA

Article

http://pubs.acs.org/journal/acsodf

Hybrid Organic-Plasmonic Nanoantennas with Enhanced Third-Harmonic Generation

Gelon Albrecht,*[,†,‡] Mario Hentschel,*[,†] Stefan Kaiser,*[,†,‡] and Harald Giessen*[,†]

[†]4th Physics Institute and Research Center SCoPE, University of Stuttgart, Pfaffenwaldring 57, 70569 Stuttgart, Germany

[‡]Max Planck Institute for Solid State Research, Heisenbergstraße 1, 70569 Stuttgart, Germany

Supporting Information

ABSTRACT: Resonantly excited plasmonic gold nanoantennas are strong sources of third-harmonic (TH) radiation. It has been shown that the response originates from large microscopic nonlinearity of the gold itself, which is enhanced by the near-field of the plasmonic nanoantenna. To further enhance this response, one can incorporate nonlinear media into the near-fields of the nanoantenna, as an additional TH source. To obtain a significant contribution from the added medium, its nonlinear susceptibility should be comparable to that of the antenna material. Many organic materials offer the necessary nonlinear susceptibility and their incorporation is possible with simple spin-coating. Furthermore, organic materials are often susceptible to photodegradation. This degradation can be used to investigate the influence of organic materials on the hybrid system. Our investigated hybrid organic plasmonic nanoantenna system consists of a gold nanorod array and poly(methyl methacrylate) as the nonlinear dielectric medium. The experiments clearly reveal two contributions to the generated TH radiation, one from the nanoantenna itself and one from the polymer. The nonlinear response of the hybrid material exceeds the response of both individual constituents and opens the path to more efficient nanoscale nonlinear light generation.

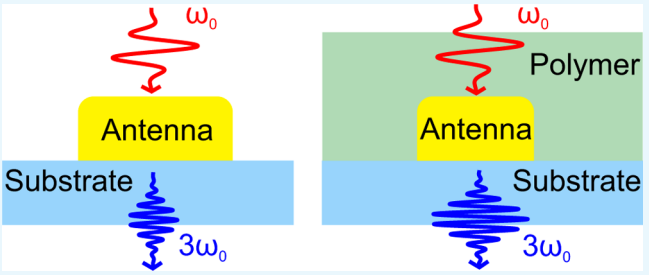

1. INTRODUCTION

Nonlinear light conversion is, despite the marginal nonlinear susceptibilities of natural materials, a common technological application, thanks to the invention of the laser.[1] Triggered by this low conversion efficiency, much effort was spent to find methods such as periodic poling[2] or materials with extremely high nonlinear susceptibilities, for example, graphene.[3] Nanostructured materials with strong optical resonances, such as metasurfaces[4,5] and plasmonic materials,[6] have been studied for enhanced nonlinear effects. In plasmonic materials, subwavelength-structured metal particles support localized surface plasmon resonances, which lead to a strong enhancement of the local electromagnetic field.[7] Owing to the superlinear relation between the exciting field and generated nonlinear field, nonlinear effects are expected to benefit strongly from the field enhancement of plasmonic resonances. Various systems from simple rod antennas[8] to split ring resonators[9] up to complicated multiresonant structures[10] have been studied in detail. All of these systems show significantly enhanced nonlinear conversion efficiency compared to that of their respective supporting substrate. However, it should be noted that the overall conversion efficiencies are small and cannot outperform bulk nonlinear optics. In fact, most systems are not meant to replace bulk nonlinear crystals but can be viewed as nanoscale nonlinear light sources with entirely different applications. In recent years, researchers have also tried to further boost the efficiency by incorporation of nonlinear inorganic dielectric materials[11−18] and organic dielectric materials.[19−21] In these systems, nonlinear dielectrics are placed within the locally enhanced electric near-field of the plasmonic structure and are thus expected to radiate stronger nonlinear signals. Several challenges became apparent by this design. First, most systems use gold as plasmonic component. Gold itself has a high nonlinear susceptibility.[22,23] Hence, all additional sources of a nonlinear signal have to compete with it. In order for this ansatz to work, one has to identify materials with comparable nonlinear susceptibilities. Second, the placement of nonlinear dielectrics, such as ITO nanoparticles, within the nanoscale volume of the enhanced near-fields is technologically challenging.[11] Third, in many systems it is extremely difficult to disentangle the different nonlinear contributions to the overall radiated signal and thus to determine the actual enhancement due to the nonlinear dielectric. This is particularly true, as the presence of the dielectric material alters the linear response of the plasmonic resonances. Especially, the resonance width is changed and thus the field enhancement, which is of utmost importance for the nonlinear conversion.[11−13] In this article, we are addressing all of these issues and find that polymers are very suited to overcome these challenges. Not only are polymers known for their large optical nonlinearities but they can also easily be applied to a nanostructured surface by spin or dip coating.

Received: April 25, 2017
Accepted: May 30, 2017
Published: June 8, 2017

ACS Publications © 2017 American Chemical Society

DOI: 10.1021/acsomega.7b00481
ACS Omega 2017, 2, 2577−2582

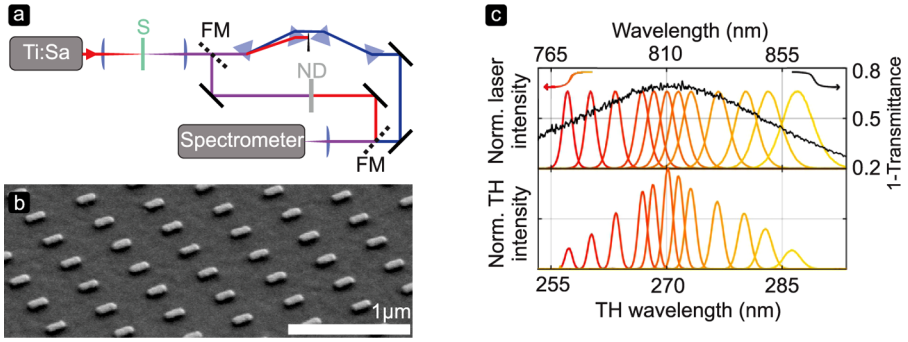

Figure 1. (a) Schematics of the spectroscopy setup. The laser impinges on the sample (S). The collected light can be sent by a flip mirror either through a neutral density filter (ND) to investigate the fundamental light or through a Fourier pulse shaper to detect only the TH. (b) A tilted SEM picture of the investigated gold-rod antenna structure. (c) Top: Measured laser spectra of the tunable TiSa laser. The pulse duration changes from 350 fs for 770 nm to 250 fs for 860 nm. The laser spectrum is tuned over the fundamental resonance of the gold antenna array (black), and the corresponding TH response is recorded. (c) Bottom: Spectra of the generated TH.

Already presented work on organic plasmonic materials mainly focuses on the nonlinear performance of the used systems.[19,20] A rigorous investigation for all influences is often not possible due to the interplay between linear and nonlinear properties. To obtain an unambiguous picture of the origin of the nonlinear response, we use controlled photodegradation of the material to disentangle the two contributions, namely, from the plasmonic nanostructures and the polymer itself. The nonlinear response can be monitored in time and shows a fluence-dependent degradation. After removing and reapplying the polymer layer, the nonlinear response nearly fully recovers the original signal strength, demonstrating a noteworthy influence of the polymer component. In addition, we can exclude any influence of a change in the linear properties by tracing the fundamental spectrum during the photodegradation. Combining the controllable off-switch and the complete comparison of all linear and nonlinear influences gives for the first time a complete picture of the origin of the nonlinearity in an organic plasmonic system.

2. RESULTS AND DISCUSSION

2.1. Third-Harmonic (TH) Spectroscopy. To demonstrate our concept, we choose TH generation (THG) from simple gold-rod nanoantennas. A tilted scanning electron micrograph (SEM) is shown in Figure 1b. The hybrid system consists of the gold-rod antennas and a homogeneous layer of poly(methyl methacrylate) (PMMA).

In the upper part of Figure 1c, the linear transmittance spectrum (measured via Fourier transform infrared spectroscopy) of a bare gold nanoantenna array over the entire tuning range is shown. The utilized laser source nicely covers the entire width of the plasmon resonance and thus allows retrieving the entire nonlinear response. One can also see the change in the spectral width of the laser pulses. The lower half of Figure 1c depicts the TH spectra generated by the gold nanoantenna array when excited by the corresponding fundamental excitations spectra (see color coding). The conversion efficiency follows the plasmonic resonance, as previously reported.[8] To easily compare the spectrally dependent conversion efficiency between different arrays, we plot in the following TH enhancement. For this, we integrate the TH spectra and plot the obtained results versus the center wavelength of the exciting fundamental laser pulse.

The reference TH both from the substrate and the substrate covered with PMMA only varies slightly with wavelength. This meets the expectations because the absorption for Suprasil as well as PMMA is nearly constant over the whole range of the exciting laser and for the generated TH range.[27] Overall, both signals are around three orders of magnitude weaker than the response from the resonant antenna array. Because of the weaker signal, the excitation power for the reference is chosen to be larger than that on the antenna field. The data is scaled afterward accordingly.

In Figure 2a, we compare the linear and nonlinear spectra of a bare nanoantenna array (red) and the hybrid gold−polymer

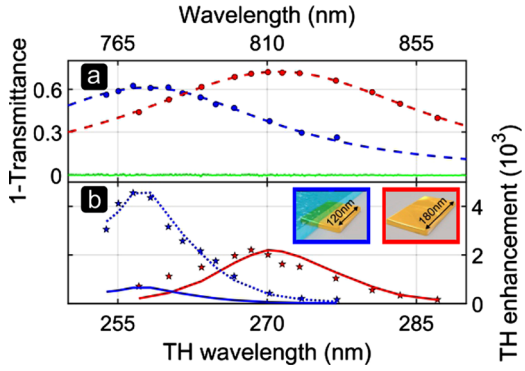

Figure 2. (a) Linear transmittance spectra for the bare gold antennas (red) and PMMA-covered antennas (blue). The lengths of the antennas differ by 60 nm to compensate for the spectral shift induced by the refractive index of PMMA. The green curve traces the transmittance of the pure PMMA, which is transparent in the investigated wavelength region. (b) The marks indicate the measured TH enhancement spectra of the hybrid system (referenced to a pure PMMA film) and bare gold system (referenced to the bare Suprasil substrate). The solid line represents the prediction of the nonharmonic oscillator model with the nonlinear parameter of the bare gold system. The model underestimates the hybrid system by a factor of 4. The dashed blue line is the nonharmonic oscillator model, with a 4 times higher nonlinear parameter.

structure (blue). The linear spectrum of the hybrid system is intentionally blue-shifted to the bare gold antenna systems to eliminate any influence from the decreased Drude damping.[13] The linear properties of the resonances are slightly different. The width of the resonance in the hybrid system is 8% smaller and the transmittance 10% larger. The increased transmittance of the hybrid system is due to the smaller gold antennas in the hybrid system. In the TH enhancement spectra (Figure 2b),

DOI: 10.1021/acsomega.7b00481
ACS Omega 2017, 2, 2577−2582

both follow linear resonance but the maximum enhancement is slightly red-shifted to the linear resonance, as reported previously.[8,13,28] For longer resonance wavelengths, we see a derivation from this redshift, which is most likely due to a varying time−bandwidth product of our excitation pulses. For absorbing polymers, three-photon fluorescence is another possible source of light in the TH wavelength range. However, fluorescence can be excluded from our experiment, as the recorded spectra show only the strong TH peak and no fluorescence background, with the characteristic asymmetric part at larger wavelengths (see Supporting Information (SI)). To predict the nonlinear response from the linear spectra, a nonharmonic oscillator model (eq 1) can be employed.[26]

$$\ddot{x} + \gamma_0\dot{x} + \omega_0^2 x - bx^3 = -\frac{e}{m}E_0 e^{-i\omega} \quad (1)$$

All parameters of the model, except the cubic perturbation, b, can be deduced from a fit to the linear spectrum. The model can then predict the shape of the TH enhancement for both hybrid and bare gold systems. The amplitude of the TH enhancement is determined by the cubic perturbation, b. The parameter, b, is therefore a measure of the local and microscopic nonlinearity of the oscillator. In the pure-gold case, this nonlinearity solely stems from the gold itself, as the nonlinearity of glass is very weak. The optical response of gold below 500 nm is affected by interband transitions[29] that could considerably change the nonlinear response. To exclude any influence we measured the THG for bare gold antennas with different resonance positions and found the nonlinear response to be well described by the nonharmonic oscillator model, assuming a constant nonlinear susceptibility (see SI). In the hybrid gold−polymer case, the nonlinearity should originate from the gold as well as from the polymer. This behavior is confirmed by the modeled TH enhancement spectra shown as solid and dashed lines in the lower half of Figure 2. We first modeled and fitted the enhancement spectrum for pure-gold antennas, shown in red, exhibiting an excellent agreement with the measured enhancement factors. Assuming the same perturbation factor, b, for the hybrid systems clearly underestimates the signals, depicted as the solid blue curve. Taking a four times larger perturbation factor leads to the spectrum shown as a dashed blue line, which is in excellent agreement with the measurement. In the framework of the nonharmonic oscillator model, the perturbation factor, b, is directly related to the nonlinear susceptibility $\chi^{(3)}$.[26] The difference in the perturbation factor therefore infers a different effective $\chi^{(3)}$ for the hybrid system. Hence, nonlinearity of the PMMA would influence the nonlinear response of the whole structure. It is important to note that other factors might also contribute to the different effective $\chi^{(3)}$. In particular, if the local electric field distributions should significantly change, the dielectric coating will certainly lead to a modified field distribution. It is therefore crucial to further investigate the underlying process and establish a more solid basis to motivate an altered $\chi^{(3)}$ and rule out other effects.

2.2. Controlled Photodegradation. To prove that PMMA is adding an additional nonlinear source, it would be ideal to switch off the PMMA contribution while leaving the gold system unchanged. By design, our hybrid system allows such an experiment in a straightforward manner. Polymers are prone to photodegradation. The investigated hybrid system exhibits a degradation threshold of 2 mW for a focus of 20 μm (see SI). For the chosen PMMA, the photodegradation leads to a strong change of the nonlinearity, whereas the linear response, that is, the refractive index, stays mostly unaffected.[30] Illuminating the hybrid system with a large enough fundamental laser intensity should therefore degrade the polymer. This will reduce the TH signal strength of the polymer whereas the TH produced by the gold is left unchanged. As the refractive index is expected to stay nearly constant, the linear response of the antenna is also expected to remain unchanged. Figure 3 depicts our measured time traces

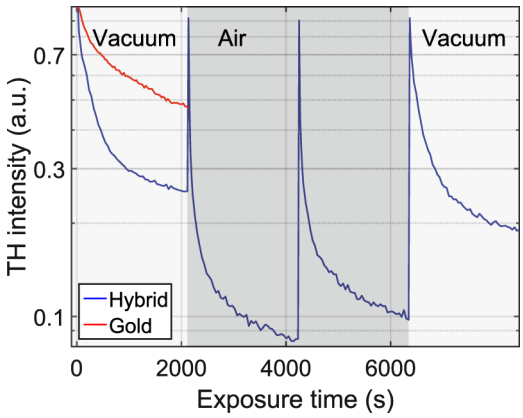

Figure 3. In blue, the decay of the TH signal of a hybrid system exposed to 10 mW average laser power at the plasmon resonance wavelength is depicted. In red, the decay of a bare gold system is drawn. After every decay cycle, PMMA is removed and the new PMMA is spin-coated on the sample. The cycles are measured in the order shown, at the same spatial point. The decay of the hybrid system is significantly faster than that of the bare gold system. Furthermore, after one cycle there is only a 10% persistent decay in the intensity of the PMMA system compared to its initial TH intensity.

of the TH signal for a 5 times higher exposure power than the degradation threshold. Measurements with further exposure powers can be found in the supplement. First, the hybrid sample is illuminated in a vacuum environment, with a pressure of roughly 10^{-5} mbar. One observes a clear decay of the radiated TH intensity, with a half-life of roughly 300 s. After an arbitrarily chosen exposure time of 2125 s, PMMA is removed in *N*-ethyl-2-pyrrolidon and acetone. Subsequently, a new layer is spin-coated to the sample. The sample is again illuminated with the same laser intensity, now in air. The TH signal strength has recovered and reaches values close yet 10% smaller than the initial values. The signal is again decaying with time, now on a much shorter time scale with a half-life time of roughly 20 s. Under these two environment conditions, the cycles are repeated. In the second cycle in air, the signal nearly perfectly matches the initial strength of the first cycle in air and again decays with a half-life time of roughly 20 s. Finally, another cycle in vacuum is performed. Again, the TH signal reaches the initial values of the two cycles in air and decays with a half-life time of roughly 300 s, as in the first cycle in vacuum. The recovery of the signal to its initial value after refreshing the PMMA layer is also clear evidence that the decayed signal originated from the polymer. The observed behavior is in complete accordance with our interpretation. The PMMA photodegrades, reducing its contribution to the nonlinear signal. The different decay time scales are also consistent with the literature. For PMMA, many photodegradation mechanisms are known, some of them involve oxygen.[31] Therefore, the exclusion of oxygen simply closes the decay channels with

DOI: 10.1021/acsomega.7b00481
ACS Omega 2017, 2, 2577−2582

oxygen and slows down the degradation. Furthermore, thermal degradation may also take place. For gold nanoantennas, a large fraction of the absorbed laser energy gets converted to heat, leading to a local heating and destruction of the surrounding polymer.[32] One open point is the reduction of the original TH signal strength. In the last three cycles, the signal recovers to the same value, yet the signal is about 10% smaller compared to that of the unexposed sample. The reason is an additional decay of the signal, stemming from the bare gold antennas. We have also measured the bare gold antennas (shown in red) and observed a clear decay in the signal strength on a significantly longer time scale of about 1500 s, which is independent of the environment. At the first glance one could expect that the decay of the bare gold should fit the difference between the polymer cycles, namely, 10%. The decay of the bare gold antennas is clearly larger. However, the degradation process for gold can be attributed to a reshaping of the particles.[33] Inside a polymer matrix, the possibilities for reshaping is limited and most likely causes an increased stability of gold in the hybrid material.

On the basis of this observation, there is a distinct difference between the THG for the hybrid system and that for the bare gold system. The THG of the hybrid system nearly completely recovers after the PMMA replacement and the decay can be cyclically reproduced. This is clear evidence that a major contribution of the THG stems from the polymer. However, we have thus far only established the major influence of the polymer on the signal. Theoretically also a change in the refractive index and thus a clear change of the linear response of the antenna could be responsible for the reduction and later recovery of the signal. To eliminate any influence of the linear properties, the linear and nonlinear properties were traced in time. Hence, multiple identical antenna fields were produced and covered with PMMA. Each field was resonantly exposed for a defined length of time. Before and after the exposure, the linear spectra of the structures were measured in a white light setup. In Figure 4a, the change of the TH intensity is depicted. As observed before, the TH intensity decays rapidly over time. If this decrease was linked to a change in the linear properties, reflecting the near-field distribution, this should be noticeable in an increased full width at half-maximum (FWHM) or a shift in the peak position of the resonance. These measurements are displayed in Figure 4. First, the peak resonance position stays constant over time. Hence, a significant change in the linear refractive index is not apparent, and the resonance is not shifting out of spectral overlap with the exciting laser. Another possibility to explain the change of the nonlinear signal with linear properties is a change in the quality factor of the resonance, which is encoded in the FWHM. With the decrease of THG, the FWHM should increase. However, there is no change visible in the FWHM in Figure 4b. With no change in the far-field spectra, no change in the near-field is to be expected. Accordingly, the field distribution in the materials system is unchanged. We have thus proven that the signal is indeed linked to the presence of the polymer and that it is not originating from a trivial change in the linear optical properties of the plasmonic resonance. Therefore, the change in the TH intensity is tied to a decrease in the effective $\chi^{(3)}$ of the hybrid structure due to photodegradation of PMMA and thus vanishing of the polymer's contribution to the radiated TH signal.

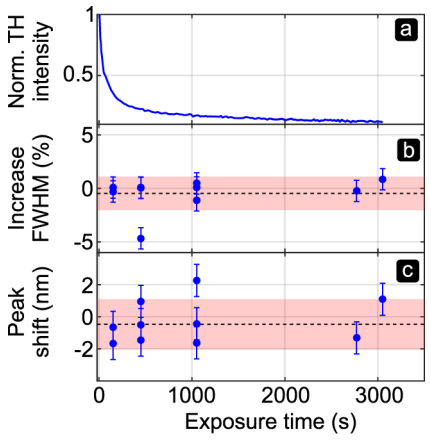

Figure 4. (a) The decrease of the TH signal with the exposure time is traced. (b) The increase in the FWHM of the linear resonance before exposure and after a certain exposure time is depicted. The dashed line indicates the mean value of the measured data and the highlighted red area is the standard derivation. (c) As second linear property the change in the peak position with the exposure time is shown. The dashed line and highlighted red area are the mean value and standard derivation, similar to the middle part.

3. CONCLUSIONS

In this work, we realized a simple hybrid organic plasmonic structure, wherein the nonlinear signal clearly originates from both constituents of the hybrid structure. To our knowledge, this is the first time that a significant influence of the dielectric $\chi^{(3)}$ on the hybrid structure's $\chi^{(3)}$ was conclusively identified. Owing to the use of an organic material, it is possible to switch off its nonlinear contribution without changing its linear properties and distinguish the antennas and the dielectric signal component. Furthermore, the overall efficiency of the hybrid structure exceeds the efficiency of its individual constituents. Finally, it provides an efficient nanoscale TH source and has potential for improvements. The PMMA could be replaced by polymers, with even higher nonlinear susceptibility.[20,34,35] Nevertheless, many polymers that we tested (P3HT, MeLPPP, and $PF_{2/6}$) have an insufficiently low damage threshold. The damage threshold of polymers for this very particular scenario is not documented and probably also not investigated very well, making a priori judgments unreliable. To improve at least the nonlinear conversion efficiency, the use of PMMA guest−host systems[36−38] may be possible because they can exceed easily the nonlinearity of the PMMA. We tested a DR1-PMMA combination, where we faced a very inhomogeneous and not reproducible response. To reduce the thermal impact caused by the gold antennas, other materials such as silicon nanoparticles[32] could be tested. Because gold shows degradation, refractory plasmonic materials, such as titanium nitride, with superior stability, can be tested as well.[33]

4. EXPERIMENTAL SECTION

4.1. Nanostructures. The gold nanostructures were fabricated via standard electron beam lithography on a UV-transparent, weakly nonlinear[22] Suprasil substrate. A tilted SEM is shown in Figure 1b. Gold was used for the antennas because it exhibits a rather narrow plasmonic resonance, leading to a high quality factor. To construct the hybrid system, the antenna arrays are coated with a nonlinear polymer, in our case, PMMA. PMMA is a standard electron beam lithography resist. Thus, it is easily accessible and obtaining homogeneous films is

DOI: 10.1021/acsomega.7b00481
ACS Omega 2017, 2, 2577−2582

straightforward. In addition, PMMA provides, in the investigated wavelength range, a rather high nonlinear refractive index.[24] It is transparent in the spectral range of the plasmon resonance and starts to absorb below 300 nm.[25] We faced significant problems with photodegradation and inhomogeneities for P3HT, DR1 in PMMA, $PF_{2/6}$, and MeLPPP that offer potentially even higher nonlinear refractive indices. All of these materials were kept under vacuum conditions as well as PMMA to minimize environmental influences. To cover the antennas, the PMMA (950 K) is spin-coated on top of the antennas and subsequently annealed (160 °C for 4 min). The resulting film is around 80 nm thick and completely covers the antennas. This polymer thickness is chosen to be sufficiently thick to fully cover that volume around the antenna in which the field enhancement is expected.[19] To minimize environmental influences, the sample is kept in a vacuum cell at 10^{-5} mbar pressure. The PMMA can easily be removed by wet chemical treatment or oxygen plasma. The hybrid as well as the bare gold antennas are designed to exhibit a plasmon resonance at 800 nm. As the polymer coating leads to a larger effective refractive index, the coated and bare gold nanoantennas need to have different sizes to be resonant around the same wavelength. For the designated resonance wavelength, this leads to the antenna length for the hybrid system and bare gold system to be 120 and 180 nm, respectively. The width of all antennas was chosen to be 50 nm, giving rise to a well-separated perpendicular resonance at 500 nm. The height of all antennas is 45 nm. Along the long axis of the antenna, the lattice constant is 500 nm, and perpendicular to it, it is 333 nm. The lattice can cause grating anomalies for the TH wavelength regime. To assure these effects to be negligible, we performed scattering matrix simulations to investigate the transmittance properties in the UV range of our sample. The simulations (see SI) show no noteworthy spectral features at the TH wavelength regime. The nanoantenna array size is 100 × 100 μm^2.

4.2. Measurement Setup. To fully verify the nonlinear response, it is necessary to sweep over the plasmon resonance of the studied samples.[8,26] We utilize a tunable TiSa Laser (Mira 9000) with a repetition rate of 75 MHz. Its tuning range from 760 to 850 nm is depicted in Figure 1c. The pulse duration decreases from 350 fs at 770 nm to 250 fs at 860 nm. Accordingly, the pulse width slightly increases. The setup is schematically shown in Figure 1a. We placed a 3 mm thick long pass filter (Schott RG 630) before the sample to remove all wavelength components shorter than 600 nm. The setup has two detection arms. One is equipped with a prism sequence used as Fourier filter to mechanically remove the fundamental wavelength component in the Fourier plane and detect only the TH signal. The other arm contains NDs to attenuate and subsequently detect the fundamental laser spectrum. Thus, this arm is used to measure the linear transmittance spectra using the tunable laser as white light source. Detection is carried out with a Peltier-cooled ultraviolet-enhanced CCD-Spectrometer. For the TH generation, the incident beam is focused to a spot size with an FWHM of 20 μm, measured by a knife-edge test. All spectroscopic measurements were conducted with an average power of 2 mW, leading to peak intensities of around 6 GW/m^2. The relative position between the beam waist and the sample was determined by maximizing the TH of a test field on each sample. For each sample, the area of highest linear absorption was used. To account for the changing pulse duration, possible chromatic aberrations, different detector efficiencies, etc. the measured TH signals are normalized to the signal generated by the bare Suprasil substrate. Similarly, the linear transmittance is normalized to the transmittance of the bare substrate.

■ ASSOCIATED CONTENT

Supporting Information

The Supporting Information is available free of charge on the ACS Publications website at DOI: 10.1021/acsomega.7b00481.

Experimental data on the absence of three-photon fluorescence, influence of the gold interband transition and fluence-dependent degradation, scattering matrix simulations regarding grating anomalies (PDF)

■ AUTHOR INFORMATION

Corresponding Authors

*E-mail: g.albrecht@pi4.uni-stuttgart.de (G.A.).
*E-mail: m.hentschel@pi4.uni-stuttgart.de (M.H.).
*E-mail: s.kaiser@fkf.mpg.de (S.K.).
*E-mail: h.giessen@pi4.uni-stuttgart.de (H.G.).

Notes

The authors declare no competing financial interest.

■ ACKNOWLEDGMENTS

We gratefully acknowledge funding from DFG SPP 1391, the BW Stiftung, the MWK BW under the Juniorprofessoren-Programm, and the Daimler und Benz Stiftung. We acknowledge funding from the ERC (Complexplas). We thank Sabine Ludwigs, Hagen Klauk, Alexander Hoyer, Florian Fischer, and Justus Back for providing different types of P3HT, Ullrich Scherf and Sybille Allard for providing $PF_{2/6}$ and MeLPPP, and Maria Farsari for providing DR1-PMMA. We express gratitude to Thomas Weiss for very helpful discussions about the scattering matrix simulation code.

■ REFERENCES

(1) Bass, M.; Franken, P. A.; Hill, A. E.; Peters, C. W.; Weinreich, G. Optical mixing. *Phys. Rev. Lett.* **1962**, *8*, 18.
(2) Jundt, D.; Magel, G.; Fejer, M.; Byer, R. Periodically poled LiNbO3 for high-effciency second-harmonic generation. *Appl. Phys. Lett.* **1991**, *59*, 2657−2659.
(3) Hendry, E.; Hale, P. J.; Moger, J.; Savchenko, A.; Mikhailov, S. Coherent nonlinear optical response of graphene. *Phys. Rev. Lett.* **2010**, *105*, No. 097401.
(4) Lee, J.; Nookala, N.; Gomez-Diaz, J. S.; Tymchenko, M.; Demmerle, F.; Boehm, G.; Amann, M.-C.; Alù, A.; Belkin, M. A. Ultrathin Second-Harmonic Metasurfaces with Record-High Nonlinear Optical Response. *Adv. Opt. Mater.* **2016**, *4*, 664−670.
(5) Lee, J.; Tymchenko, M.; Argyropoulos, C.; Chen, P.-Y.; Lu, F.; Demmerle, F.; Boehm, G.; Amann, M.-C.; Alù, A.; Belkin, M. A. Giant nonlinear response from plasmonic metasurfaces coupled to intersubband transitions. *Nature* **2014**, *511*, 65−69.
(6) Kauranen, M.; Zayats, A. V. Nonlinear plasmonics. *Nat. Photonics* **2012**, *6*, 737−748.
(7) Novotny, L.; van Hulst, N. Antennas for light. *Nat. Photonics* **2011**, *5*, 83−90.
(8) Metzger, B.; Hentschel, M.; Lippitz, M.; Giessen, H. Third-harmonic spectroscopy and modeling of the nonlinear response of plasmonic nanoantennas. *Opt. Lett.* **2012**, *37*, 4741−4743.
(9) Linden, S.; Niesler, F.; Förstner, J.; Grynko, Y.; Meier, T.; Wegener, M. Collective effects in second-harmonic generation from split-ring-resonator arrays. *Phys. Rev. Lett.* **2012**, *109*, No. 015502.
(10) Aouani, H.; Navarro-Cia, M.; Rahmani, M.; Sidiropoulos, T. P.; Hong, M.; Oulton, R. F.; Maier, S. A. Multiresonant broadband optical

DOI: 10.1021/acsomega.7b00481
ACS Omega 2017, 2, 2577−2582

antennas as effcient tunable nanosources of second harmonic light. *Nano Lett.* **2012**, *12*, 4997−5002.
(11) Hentschel, M.; Metzger, B.; Knabe, B.; Buse, K.; Giessen, H. Linear and nonlinear optical properties of hybrid metallic-dielectric plasmonic nanoantennas. *Beilstein J. Nanotechnol.* **2016**, *7*, 111−120.
(12) Linnenbank, H.; Grynko, Y.; Förstner, J.; Linden, S. Second harmonic generation spectroscopy on hybrid plasmonic/dielectric nanoantennas. *Light: Sci. Appl.* **2016**, *5*, No. e16013.
(13) Metzger, B.; Hentschel, M.; Schumacher, T.; Lippitz, M.; Ye, X.; Murray, C. B.; Knabe, B.; Buse, K.; Giessen, H. Doubling the effciency of third harmonic generation by positioning ITO nanocrystals into the hot-spot of plasmonic gap-antennas. *Nano Lett.* **2014**, *14*, 2867−2872.
(14) Niesler, F. B. P.; Feth, N.; Linden, S.; Niegemann, J.; Gieseler, J.; Busch, K.; Wegener, M. Second-harmonic generation from split-ring resonators on a GaAs substrate. *Opt. Lett.* **2009**, *34*, 1997−1999.
(15) Pu, Y.; Grange, R.; Hsieh, C.-L.; Psaltis, D. Nonlinear optical properties of core-shell nanocavities for enhanced second-harmonic generation. *Phys. Rev. Lett.* **2010**, *104*, No. 207402.
(16) Jais, P. M.; von Bilderling, C.; Bragas, A. V. Plasmon-enhanced second harmonic generation in semiconductor quantum dots close to metal nanoparticles. *Pap. Phys.* **2011**, *3*, No. 030002.
(17) Grinblat, G.; Rahmani, M.; Cortés, E.; Caldarola, M.; Comedi, D.; Maier, S. A.; Bragas, A. V. High-effciency second harmonic generation from a single hybrid zno nanowire/au plasmonic nano-oligomer. *Nano Lett.* **2014**, *14*, 6660−6665.
(18) Aouani, H.; Rahmani, M.; Navarro-Cía, M.; Maier, S. A. Third-harmonic-upconversion enhancement from a single semiconductor nanoparticle coupled to a plasmonic antenna. *Nat. Nanotechnol.* **2014**, *9*, 290−294.
(19) Chen, K.; Durak, C.; Heflin, J.; Robinson, H. D. Plasmon-enhanced second-harmonic generation from ionic self-assembled multilayer films. *Nano Lett.* **2007**, *7*, 254−258.
(20) Ren, F.; Wang, X.; Li, Z.; Luo, J.; Jang, S.-H.; Jen, A. K.-Y.; Wang, A. X. Enhanced third harmonic generation by organic materials on high-Q plasmonic photonic crystals. *Opt. Express* **2014**, *22*, 20292−20297.
(21) Cai, W.; Vasudev, A. P.; Brongersma, M. L. Electrically controlled nonlinear generation of light with plasmonics. *Science* **2011**, *333*, 1720−1723.
(22) Boyd, R. W. *Nonlinear Optics*, 2nd ed.; Academic Press, 2003.
(23) Bloembergen, N.; Burns, W.; Matsuoka, M. Reflected third harmonic generated by picosecond laser pulses. *Opt. Commun.* **1969**, *1*, 195−198.
(24) Hussan, R. M.; Mahdi, Z. F.; Faris, R. A. Nonlinear Optical Properties of PMMA Composites Using Z-Scan Technique. *Iraqi J. Sci.* **2013**, *12*, 27−35.
(25) Zidan, H.; Abu-Elnader, M. Structural and optical properties of pure PMMA and metal chloride-doped PMMA films. *Phys. B* **2005**, *355*, 308−317.
(26) Hentschel, M.; Utikal, T.; Giessen, H.; Lippitz, M. Quantitative modeling of the third harmonic emission spectrum of plasmonic nanoantennas. *Nano Lett.* **2012**, *12*, 3778−3782.
(27) Niesler, F. B.; Feth, N.; Linden, S.; Wegener, M. Second-harmonic optical spectroscopy on split-ring-resonator arrays. *Opt. Lett.* **2011**, *36*, 1533−1535.
(28) Zuloaga, J.; Nordlander, P. On the energy shift between near-field and far-field peak intensities in localized plasmon systems. *Nano Lett.* **2011**, *11*, 1280−1283.
(29) Lässer, R.; Smith, N. V. Interband optical transitions in gold in the photon energy range 2−25 eV. *Solid State Commun.* **1981**, *37*, 507−509.
(30) Wochnowski, C. UV-laser-based fabrication of a planar, polymeric Bragg-structure. *Opt. Laser Technol.* **2009**, *41*, 734−740.
(31) Mitsuoka, T.; Torikai, A.; Fueki, K. Wavelength sensitivity of the photodegradation of poly (methyl methacrylate). *J. Appl. Polym. Sci.* **1993**, *47*, 1027−1032.
(32) Caldarola, M.; Albella, P.; Cortés, E.; Rahmani, M.; Roschuk, T.; Grinblat, G.; Oulton, R. F.; Bragas, A. V.; Maier, S. A. Non-plasmonic nanoantennas for surface enhanced spectroscopies with ultra-low heat conversion. *Nat. Commun.* **2015**, *6*, No. 7915.
(33) Gui, L.; Bagheri, S.; Strohfeldt, N.; Hentschel, M.; Zgrabik, C. M.; Metzger, B.; Linnenbank, H.; Hu, E. L.; Giessen, H. Nonlinear Refractory Plasmonics with Titanium Nitride Nanoantennas. *Nano Lett.* **2016**, *16*, 5708−5713.
(34) Carter, G.; Thakur, M.; Chen, Y.; Hryniewicz, J. Time and wavelength resolved nonlinear optical spectroscopy of a polydiacetylene in the solid state using picosecond dye laser pulses. *Appl. Phys. Lett.* **1985**, *47*, 457−459.
(35) Li, Z.; Ensley, T. R.; Hu, H.; Zhang, Y.; Jang, S.-H.; Marder, S. R.; Hagan, D. J.; Van Stryland, E. W.; Jen, A. K.-Y. Conjugated Polycyanines: A New Class of Materials with Large Third-Order Optical Nonlinearities. *Adv. Opt. Mater.* **2015**, *3*, 900−906.
(36) D'Amore, F.; Lanata, M.; Pietralunga, S. M.; Gallazzi, M. C.; Zerbi, G. Enhancement of PMMA nonlinear optical properties by means of a quinoid molecule. *Opt. Mater.* **2004**, *24*, 661−665.
(37) Liang, J.; Zhou, X. Q. Application of continuous-wave laser Z-scan technique to photoisomerization. *J. Opt. Soc. Am. B* **2005**, *22*, 2468−2471.
(38) Singer, K.; Kuzyk, M.; Holland, W.; Sohn, J.; Lalama, S.; Comizzoli, R.; Katz, H.; Schilling, M. Electro-optic phase modulation and optical second-harmonic generation in corona-poled polymer films. *Appl. Phys. Lett.* **1988**, *53*, 1800−1802.

DOI: 10.1021/acsomega.7b00481
ACS Omega 2017, 2, 2577−2582